

Spectrally resolved NOON state interference

Rui-Bo Jin^{1,2}, Ryosuke Shimizu³, Takafumi Ono^{2,4,5}, Mikio Fujiwara²,
Guang-Wei Deng⁶, Qiang Zhou^{6,*}, Masahide Sasaki^{2,†} and Masahiro Takeoka^{2,7‡}

¹*Hubei Key Laboratory of Optical Information and Pattern Recognition,
Wuhan Institute of Technology, Wuhan 430205, China*

²*National Institute of Information and Communications Technology,
4-2-1 Nukui-Kitamachi, Koganei, Tokyo 184-8795, Japan*

³*University of Electro-Communications, 1-5-1 Chofugaoka, Chofu, Tokyo 182-8585, Japan*

⁴*Faculty of Engineering and Design, Kagawa University,
2217-20, Hayashi-cho, Takamatsu, Kagawa Japan*

⁵*JST, PRESTO, 4-1-8 Honcho, Kawaguchi, Saitama, 332-0012, Japan*

⁶*Institute of Fundamental and Frontier Sciences and School of Optoelectronic Science and Engineering,
University of Electronic Science and Technology of China, Chengdu 610054, China and*

⁷*Keio University, 3-14-1 Hiyoshi, Kohoku, Yokohama, Kanagawa 223-8522, Japan*

(Dated: January 6, 2022)

NOON state interference (NOON-SI) is a powerful tool to improve the phase sensing precision, and plays an important role in quantum measurement. In most of the previous NOON-SI experiments, the measurements were performed in time domain where the spectral information of the involved photons was integrated and lost during the measurement. In this work, we experimentally measured the joint spectral intensities (JSIs) at different positions of the interference patterns in both time and frequency domains. It was observed that the JSIs were phase-dependent and show odd (even)-number patterns at 0 (π) phase shift; while no interference appeared in time domain measurement, the interference pattern clearly appeared in frequency domain. To our best knowledge, the latter is the first observation of the spectrally resolved NOON state interference, which provides alternative information that cannot be extracted from the time-domain measurement. To explore its potential applications, we considered the interferometric sensing with our setup. From the Fisher information-based analysis, we show that the spectrally resolved NOON-SI has a better performance at non-zero-delay position than its non-spectrally resolved counterpart. The spectrally resolved NOON-SI scheme may be useful for quantum metrology applications such as quantum phase sensing, quantum spectroscopy, and remote synchronization.

Introduction Multi-photon entanglement and multi-photon interference are useful nonclassical resources in quantum information applications. In particular, the so-called NOON state interference (NOON-SI) is a powerful tool to improve the phase sensing precision. NOON state is an entangled state with N photons occupying either one of two optical modes (e.g., polarization modes or path modes): $\frac{1}{\sqrt{2}}(|N0\rangle + |0N\rangle)$ [1–3]. NOON-SI is a powerful tool to improve the phase sensing precision to Heisenberg limit of $\Delta\phi = 1/N$, much higher than the shot noise limit of $\Delta\phi = 1/\sqrt{N}$, which is precision limit of the classical interferometer, e.g., the Mach-Zehnder interferometer (MZI) [4]. NOON-SI has been widely used in super-resolving phase measurements [5–10], quantum lithography [1], quantum microscopy [11, 12], quantum spectroscopy [13] and error correction [14].

Most of the previous NOON-SI experiments were measured in time domain [1–14], i.e., the interference patterns are obtained by recording the coincidence counts as a function of the temporal delay. However, the conjugate parameter of time, i.e., the spectral information of the involved photons was integrated and lost during the time-domain measurement. The knowledge of the spectral correlations of the interfering photons can reveal some important information about the interference visibility [15, 16]. Therefore, it is very valuable to explore

such spectral information. But in the past the spectral correlation content could not be observed, partially due to the long acquisition times required when measuring spectral correlations using two tunable bandpass filters [17]. Recently, a new technique for measuring spectral correlations in a Hong-Ou-Mandel (HOM) interference [18] was presented by Gerrits, et al [16, 19, 20]. This technique has the merits of short measurement time and high spectral resolution, and therefore allows measuring and analyzing the spectral correlations from a HOM interference [16, 19, 20]. This technique also make it possible to observe the joint spectral information during the NOON-SI.

In this work, we apply the state-of-art spectral correlation measurement technique in the NOON-SI, and measure the joint spectral intensities (JSIs) at different positions of the interference. We observe the interference pattern in the frequency domain clearly, while no interference appears in the time-domain measurement. This implies that some new spectral information was indeed observed, although it was integrated and lost during the time-domain measurement.

Experiment and results The experimental setup for the NOON-SI is shown in Fig.1(a). Picosecond laser pulses (pulse repetition frequency = 76 MHz, wavelength = 792 nm, temporal duration ~ 2 ps) from a mode-locked

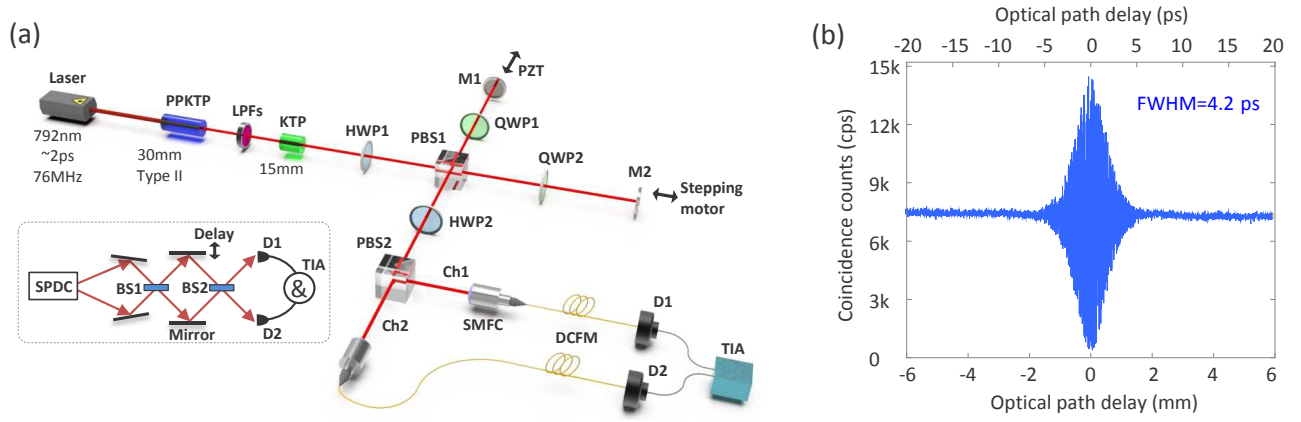


FIG. 1. (a): The experimental setup for NOON-SI using polarization-mode. LPF=long pass filter, HWP=half wave plate, M=mirror, QWP=quarter wave plate, PZT=piezo-electric linear actuator, PBS=polarization beam splitter, SMFC=single-mode fiber coupler, DCFM=dispersion compensation fiber module, TIA=time interval analyzer. The inset depicts a standard configuration of the NOON-SI using path-mode. BS=beam splitter. (b): The NOON-SI pattern measured in time domain by scanning a stepping motor with a step length of $4 \mu\text{m}$.

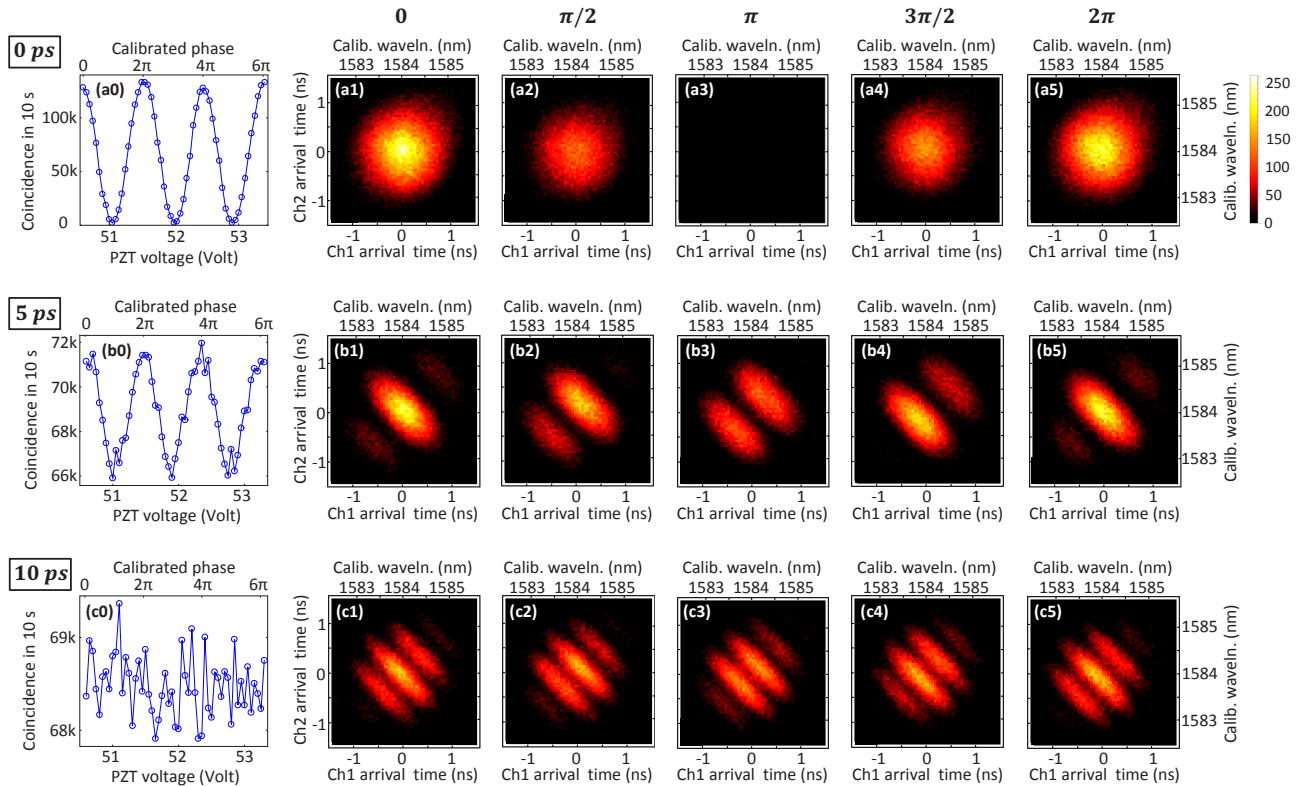


FIG. 2. (a0, b0, c0): The experimental NOON-SI pattern measured in time domain by scanning a PZT with a step length several nm, when fix the stepping motor at the delay time of 0 ps, 5 ps and 10 ps, respectively. The visibility is $97.09 \pm 0.03\%$, $3.53 \pm 0.50\%$ and 0% (a1-a5, b1-b5, c1-c5): The measured JSIs at different phase delay from 0 to 2π in (a0, b0, c0).

Titanium sapphire laser pump a 30-mm-long PPKTP crystal with a poling period of $46.1 \mu\text{m}$ for type-II group-velocity-matched SPDC [17, 21]. The down converted photons, i.e., the signal and idler photons, have orthogonal polarizations and degenerate wavelengths at 1584 nm. To temporally overlap the signal and idler,

the down converted biphotons pass through a 15-mm-long KTP crystal. Then, the biphotons are mixed on a half wave plate (HWP1, at 22.5°), which functions similarly as a beamsplitter in the NOON-SI using path-mode (BS1 in the inset of Fig. 1(a)). After the biphotons are separated by a polarization beam splitter (PBS1), they are sent to

a time delay system, which is composed of two quarter wave plates (QWP1 and QWP2, at 45°) and two mirrors. One of the mirrors (M1) is set on a PZT to achieve a scanning step in the order of nm, while the other one (M2) is on a stepping motor to realize a scanning step of μm . Then, the biphotons are mixed again on the second half wave plate (HWP2, at 22.5°), which functions as the BS2 in the inset. Finally, the biphotons are separated by PBS2 and collected into two channels of single-mode fibers (Ch1 and Ch2), which is connected to a dispersion spectrometer [16, 19, 20, 22, 23], composed of a dispersion compensation fiber module (DCFM), two superconducting nanowire single-photon detectors (SNSPDs) [24] and a time interval analyzer (TIA). The DCFM has a dispersion of 125.0 ps/km/nm (full dispersion of 941 ps/nm) and an insertion loss of 5.2 dB. The SNSPDs have detection efficiencies around 70% with dark counts less than 1 kHz. Assuming a system jitter of 100 ps, the resolution of our fiber spectrometer is estimated as 0.11 nm. To keep the phase stability in the interference, we set the time delay system in an enclosed paper box to avoid the air flow, such that the phase stability can be maintained for more than 5 minutes.

The PPKTP crystal is pumped with a power of 50 mW. With the insertion of DCFM, we obtain an average singles count rate of about 200 kcps, and a two-fold coincidence count rate of about 7 kcps. First, we measure the NOON-SI in time domain, i.e., scan the time delay using a stepping motor and record the coincidence counts. Fig. 1(b) shows the measured interference pattern with a full-width-at-half-maximum (FWHM) of 4.2 ps (1.3 nm). Then, we characterize the NOON-SI in spectral domain, i.e., the JSI of the biphotons in Ch1 and Ch2 was measured at different delay time. We focus on three delay time: 0 ps, 5 ps and 10 ps, by moving the stepping motor as the coarse adjustment and scan the PZT as the fine adjustment.

Figure 2(a0) shows the interference pattern at 0 ps. By driving the PZT with a voltage from 50 V to 53 V, the resultant relative phase delay is about 6π . The interference visibility in Fig. 2(a0) is $97.09 \pm 0.03\%$ and the oscillation period is 792 nm (0.462 fs), half of the biphoton's wavelength. Then, we measure the JSI using the dispersion spectrometer. Figure 2(a1-a5) shows the measured JSIs at the relative phase from 0 to 2π with a step of $\pi/2$. The horizontal (vertical) axis is the arrival time of the photons in Ch1 (Ch2). The arrival time is ranging from -1.5 ns to 1.5 ns, and the corresponding wavelength is from 1582 nm to 1586 nm. Each figure was accumulated for 60 seconds. The JSI at 0 (2π) is the brightest and at π is the darkest. The JSI in Fig. 2(a1) is equal to the JSI of the biphoton source.

Figure 2(b0) shows the measured coincidence counts as a function of time delay at 5 ps. The visibility is $3.53 \pm 0.50\%$, which can also be confirmed in Fig. 1(b). Figure 2(b1-b5) shows the measured JSIs at the phase of

0, $\frac{\pi}{2}$, π , $\frac{3\pi}{2}$, and 2π in Fig. 2(b0). It can be observed clearly that the distribution of the JSIs is splitting along the diagonal axis. The JSI is phase sensitive, i.e., the distribution in the JSI is different for different phases. At $\frac{\pi}{2}$, the up-right section is brighter, while at $\frac{3\pi}{2}$, the down-left section is brighter.

Figure 2(c0) shows the temporal interference pattern at the time delay of 10 ps. The visibility is almost zero in Fig. 2(c0), as also confirmed in Fig. 1(b). Figure 2(c1-c5) shows the measured JSIs at the phase of 0, $\frac{\pi}{2}$, π , $\frac{3\pi}{2}$, and 2π in Fig. 2(c0). It can be noticed that the JSI is separated into odd-number sections at 0 (2π), and even-number sections at π . It can be concluded that when the time-domain interference visibility is almost zero, the interference patterns in the spectral domain are still very clear.

Theoretical analysis The experimental results in Fig. 2 is well explained in theory. Assume the signal and idler photons from the SPDC has a joint spectral amplitude (JSA) of $f(\omega_s, \omega_i)$, where ω is the angular frequency; the subscripts s and i denote the signal and idler. For simplicity, we further assume the JSA has the exchanging symmetry of $f(\omega_s, \omega_i) = f(\omega_i, \omega_s)$. After a long calculation using multi-spectral-mode theory [13, 25], the two-fold coincidence probability P as a time delay τ in a NOON-SI can be described by

$$P(\tau) = \frac{1}{2} \int_0^\infty \int_0^\infty d\omega_s d\omega_i |f(\omega_s, \omega_i)|^2 [1 + \cos(\omega_s + \omega_i)\tau]. \quad (1)$$

The JSI $I(\omega_s, \omega_i, \tau)$ during the NOON-SI can be written as

$$I(\omega_s, \omega_i, \tau) = \frac{1}{2} |f(\omega_s, \omega_i)|^2 [1 + \cos(\omega_s + \omega_i)\tau]. \quad (2)$$

Using the parameters of the pump laser and the PPKTP crystal, we can calculate the JSA. With the JSA, the time-domain interference patterns in Fig. 1(b) and Fig. 2(a0, b0, c0) can be simulated using Eq.(1). The frequency-domain interference patterns in Fig. 2(a1-a5, b1-b5, c1-c5) can be simulated by using Eq.(2).

Figure 3 shows the simulated results. In Fig. 3(a0, b0, c0), the visibility are 100%, 3.8% and 0.006%, which correspond well with the experimental results in Fig. 2(a0, b0, c0). Figure 3(a1-a5, b1-b5, c1-c5) shows the simulated JSIs at different phase delay from 0 to 2π in (a0, b0, c0). The measured JSIs are consistent with the simulated ones. The experimentally measured JSIs are "fatter" than the simulated JSIs, since the resolution of the fiber spectral meter is limited.

Discussion We compare the traditional *non-spectrally resolved (NSR)* NOON-SI and the *spectrally resolved* NOON-SI in our scheme by analyzing the Fisher information, which has been widely used to evaluate the phase sensing ability of the NOON-SI [26]. As shown in the **Supplementary Materials**, the Fisher information

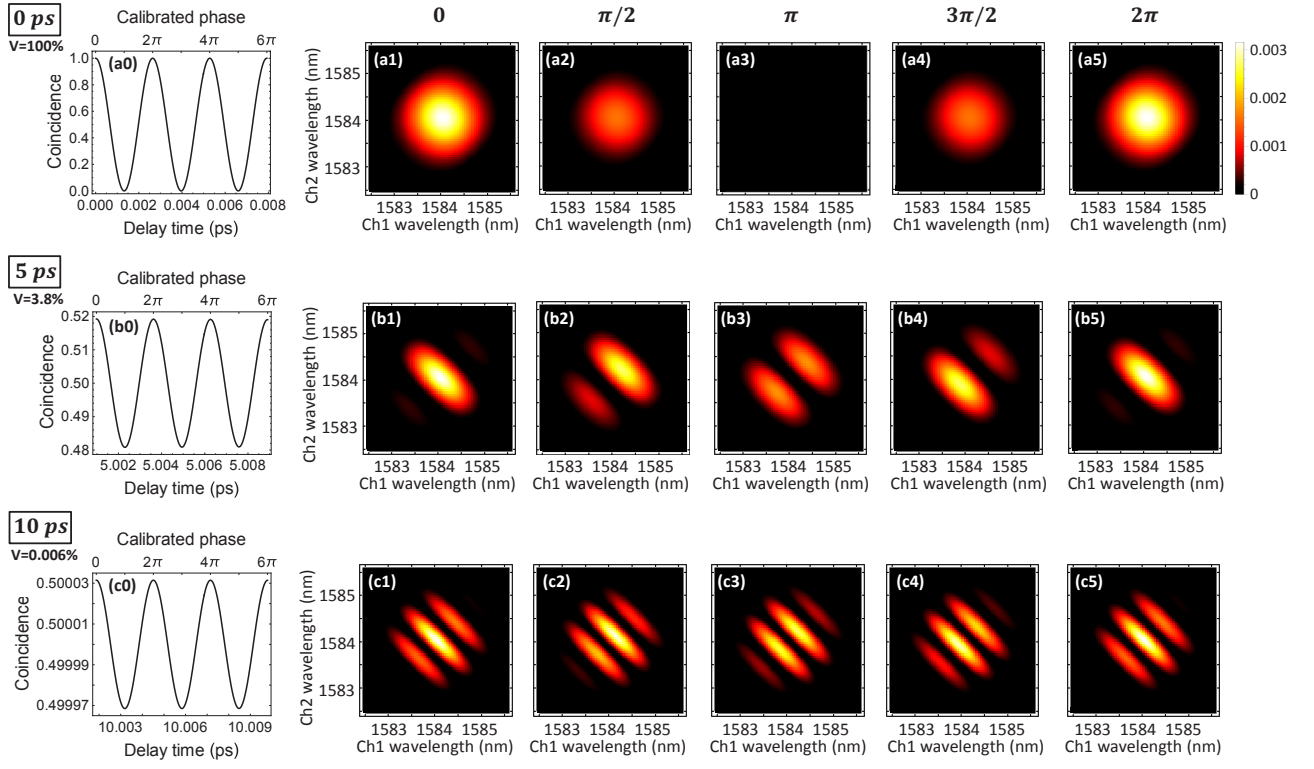


FIG. 3. (a0, b0, c0): The theoretically simulated NOON-SI pattern in time domain at the delay time of 0 ps, 5 ps and 10 ps, respectively. The visibilities are 100%, 3.8% and 0.006%. (a1-a5, b1-b5, c1-c5): The simulated JSIs at different phase delay from 0 to 2π in (a0, b0, c0).

for the *non-spectrally resolved* NOON-SI (F_{NSR}) can be calculated as:

$$F_{NSR}(\tau) = \frac{[P'_{NSR}(\tau)]^2}{P_{NSR}(\tau)[1 - P_{NSR}(\tau)]}, \quad (3)$$

where $P_{NSR}(\tau) = P(\tau)$ and P'_{NSR} is the differentiation of P_{NSR} with respect to the time τ . Fisher information for the *spectrally resolved* NOON-SI (F_{SR}) is

$$F_{SR}(\tau) = \int_0^\infty \int_0^\infty |f(\omega_s, \omega_i)|^2 \times (\omega_s + \omega_i)^2 d\omega_s d\omega_i. \quad (4)$$

With these two equations and the theoretical $f(\omega_s, \omega_i)$, we simulated F_{NSR} (in gray) and F_{SR} (in red) in Fig. 4. It is noteworthy that F_{SR} equals to the maximal value of F_{NSR} and does not degrade in delay. This feature implies that the spectrally resolved techniques enable the acquisition of higher Fisher information in wider range of delay time. This advantage is very useful for time or phase estimation in wide range.

It is interesting to compare this spectrally resolved NOON-SI with the result in the spectrally resolved HOM interference in Refs. [16, 19, 20]. In the NOON-SI, the JSI is splitting along the anti-diagonal direction, while the JSI is splitting along the diagonal direction in the HOM interference. This difference is result from

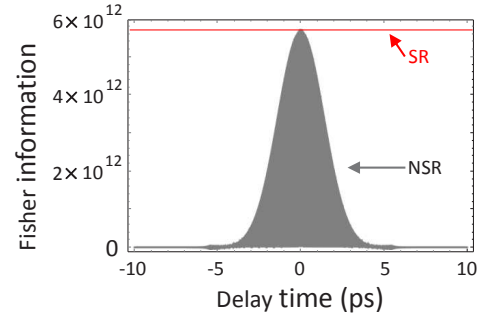


FIG. 4. Fisher information for the *non-spectrally resolved* NOON-SI (in gray) and the *spectrally resolved* NOON-SI (in red).

the facts that the NOON-SI is a sum-frequency interference, which is described in Eq.(1), while the HOMI is a difference-frequency interference, as explained in Refs. [3, 13, 16, 19, 20]. It can be observed that the distribution of the JSI is changing at different phase delay. This phase dependent feature is totally different from the case of HOM interference [16, 19, 20], which is phase independent. The spectrally resolved HOM interference has been applied for the situation in which the phase insensitivity is required, e.g., the generation and distribution of frequency-entangled qudits [20], efficient

quantum-optical coherence tomography [27].

We noticed the recent report on the spectrally-resolved quantum white-light interferometry (WLI) for optical chromatic dispersion measurement, which has a better precision than the classical WLI and can be used for absolute parameter determination [28]. In Ref. [28] only one spectrometer was utilized, i.e., one-dimensional spectrally-resolved. In contrast, our measurement are two-dimensional spectrally resolved, where two spectrometers are utilized to measure the spectral correlation between the signal and idler photons. This two dimensional spectral resolving technique may also has the potential for higher precision parameter estimation in wider range in the future.

It is important to discuss the feasibility of the future applications. The interference visibility is almost 0 in time domain at 10 ps in Fig.2(c0), however, the visibility in spectral domain in Fig.2(c1-c5) is still very high. This implies that the spectral measurement can exploit some new information that has never been measured in the time domain. This extra spectral information might be an important supplementary to the time-domain information, and might be used for promising applications, such as remote synchronization [29], quantum spectroscopy [30, 31] and quantum metrology [32, 33] in the future.

Conclusion We have experimentally and theoretically demonstrated spectrally resolved NOON-SI with a spontaneous parametric down conversion source at 1584 nm wavelength. It was confirmed that, while there is no interference in time domain, the interference visibility in spectral domain is still very high. The spectrally resolved NOON-SI has a higher Fisher information than the non-spectrally resolved NOON-SI at the position far from the interference center, therefore has a better performance for time or phase estimation in a wider range. This spectrally resolved NOON-SI scheme may be applied for remote synchronization, absolute parameter estimation, quantum spectroscopy, and quantum metrology.

Acknowledgements The authors thank Thomas Gerrits and Kentaro Wakui for helpful discussions. This work is partially supported by the ImPACT Program of Council for Science, Technology and Innovation (Cabinet Office, Government of Japan), by the National Key R&D Program of China (Grant No. 2018YFA0307400), the National Natural Science Foundations of China (Grant Nos. 91836102, 11704290, 12074299, 61775025, 12074058), and by a fund from the Educational Department of Hubei Province, China (Grant No. D20161504).

* zhouqiang@uestc.edu.cn

† psasaki@nict.go.jp

- ‡ Takeoka@uec.ac.jp
- [1] A. N. Boto, P. Kok, D. S. Abrams, S. L. Braunstein, C. P. Williams, and J. P. Dowling, *Phys. Rev. Lett.* **85**, 2733 (2000).
 - [2] K. Edamatsu, R. Shimizu, and T. Itoh, *Phys. Rev. Lett.* **89**, 213601 (2002).
 - [3] V. Giovannetti, L. Maccone, J. H. Shapiro, and F. N. C. Wong, *Phys. Rev. Lett.* **88**, 183602 (2002).
 - [4] V. Giovannetti, S. Lloyd, and L. Maccone, *Science* **306**, 1330 (2004).
 - [5] M. W. Mitchell, J. S. Lundeen, and A. M. Steinberg, *Nature* **429**, 161 (2004).
 - [6] P. Walther, J.-W. Pan, M. Aspelmeyer, R. Ursin, S. Gasparoni, and A. Zeilinger, *Nature* **429**, 158 (2004).
 - [7] T. Nagata, R. Okamoto, J. L. O'Brien, K. Sasaki, and S. Takeuchi, *Science* **316**, 726 (2007).
 - [8] I. Afek, O. Ambar, and Y. Silberberg, *Science* **328**, 879 (2010).
 - [9] S. Slussarenko, M. M. Weston, H. M. Chrzanowski, L. K. Shalm, V. B. Verma, S. W. Nam, and G. J. Pryde, *Nat. Photon.* **11**, 700 (2017).
 - [10] Z.-Y. Zhou, S.-L. Liu, S.-K. Liu, Y.-H. Li, D.-S. Ding, G.-C. Guo, and B.-S. Shi, *Phys. Rev. Appl.* **7**, 064025 (2017).
 - [11] T. Ono, R. Okamoto, and S. Takeuchi, *Nat. Commun.* **4**, 2426 (2013).
 - [12] Y. Israel, S. Rosen, and Y. Silberberg, *Phys. Rev. Lett.* **112**, 103604 (2014).
 - [13] R.-B. Jin and R. Shimizu, *Optica* **5**, 93 (2018).
 - [14] M. Bergmann and P. van Loock, *Phys. Rev. A* **94**, 012311 (2016).
 - [15] P. J. Mosley, *Generation of Heralded Single Photons in Pure Quantum States*, Ph.D. thesis, University of Oxford (2007).
 - [16] T. Gerrits, F. Marsili, V. B. Verma, L. K. Shalm, M. Shaw, R. P. Mirin, and S. W. Nam, *Phys. Rev. A* **91**, 013830 (2015).
 - [17] R.-B. Jin, R. Shimizu, K. Wakui, H. Benichi, and M. Sasaki, *Opt. Express* **21**, 10659 (2013).
 - [18] C. K. Hong, Z. Y. Ou, and L. Mandel, *Phys. Rev. Lett.* **59**, 2044 (1987).
 - [19] R.-B. Jin, T. Gerrits, M. Fujiwara, R. Wakabayashi, T. Yamashita, S. Miki, H. Terai, R. Shimizu, M. Takeoka, and M. Sasaki, *Opt. Express* **23**, 28836 (2015).
 - [20] R.-B. Jin, R. Shimizu, M. Fujiwara, M. Takeoka, R. Wakabayashi, T. Yamashita, S. Miki, H. Terai, T. Gerrits, and M. Sasaki, *Quantum Sci. Technol.* **1**, 015004 (2016).
 - [21] F. König and F. N. C. Wong, *Appl. Phys. Lett.* **84**, 1644 (2004).
 - [22] M. Avenhaus, A. Eckstein, P. J. Mosley, and C. Silberhorn, *Opt. Lett.* **34**, 2873 (2009).
 - [23] T. Gerrits, M. J. Stevens, B. Baek, B. Calkins, A. Lita, S. Glancy, E. Knill, S. W. Nam, R. P. Mirin, R. H. Hadfield, R. S. Bennink, W. P. Grice, S. Dorenbos, T. Zijlstra, T. Klapwijk, and V. Zwiller, *Opt. Express* **19**, 24434 (2011).
 - [24] S. Miki, T. Yamashita, H. Terai, and Z. Wang, *Opt. Express* **21**, 10208 (2013).
 - [25] Z.-Y. J. Ou, *Multi-photon quantum interference* (Springer, 2007).
 - [26] G. Y. Xiang, H. F. Hofmann, and G. J. Pryde, *Sci. Rep.* **3**, 2684 (2013).
 - [27] P. Yepiz-Graciano, A. M. A. Martinez, D. Lopez-Mago, H. Cruz-Ramirez, and A. B. U'Ren, *Photon. Res.* **8**, 1023

- (2020).
- [28] F. Kaiser, P. Vergyris, D. Aktas, C. Babin, L. Labont, and S. Tanzilli, *Light Sci. Appl.* **7**, 17163 (2018).
 - [29] R. Quan, Y. Zhai, M. Wang, F. Hou, S. Wang, X. Xiang, T. Liu, S. Zhang, and R. Dong, *Sci. Rep.* **6**, 30453 (2016).
 - [30] H. T. Dinani, M. K. Gupta, J. P. Dowling, and D. W. Berry, *Phys. Rev. A* **93**, 063804 (2016).
 - [31] R. Whittaker, C. Erven, A. Neville, M. Berry, J. L. O'Brien, H. Cable, and J. C. F. Matthews, *New J. Phys.* **19**, 023013 (2017).
 - [32] J. P. Dowling, *Contemp. Phys.* **49**, 125 (2008).
 - [33] M. A. Taylor and W. P. Bowen, *Phys. Rep.* **615**, 1 (2016).

SUPPLEMENTARY MATERIALS

1: FISHER INFORMATION ANALYSIS

Here we derive the Fisher information for non-spectrally-resolved NOON-SI and spectrally-resolved NOON-SI. Fisher information determines the minimum detectable time (τ) in the measurement, which is calculated by the set of time dependent measurement probabilities. For spectrally resolved measurement, the probability densities at certain frequencies of signal (ω_s) and idler (ω_i) photons corresponds to the joint spectrum intensities. On the other hand, for non-spectrally-resolved measurement, the probabilities are given by integrating the joint spectrum intensities over ω_s and ω_i . Thus the Fisher information for spectrally resolved measurement is different from the one for non-spectrally resolved measurement. In the following, we will derive the Fisher information for each cases.

1.1: Fisher information for non-spectrally-resolved NOON-SI

In general, Fisher information is calculated from the set of time dependent measurement probabilities as given by:

$$F(\tau) \equiv \sum_k p_k(\tau) \left(\frac{\partial[\ln p_k(\tau)]}{\partial\tau} \right)^2 = \sum_k \frac{[p'_k(\tau)]^2}{p_k(\tau)}, \quad (\text{S1})$$

where p_k is the probability of the k^{th} possible measurement, and ' represents the first order differentiation with respect to the time τ . As discussed in [26], in the case of a single measurement with a probability of $p(\tau)$, the Fisher information can be given by the contribution of the single fringe to the sum in Eq. (S1), combined with the information from its null fringe:

$$F(\tau) = p(\tau) \left(\frac{\partial[\ln p(\tau)]}{\partial\tau} \right)^2 + [1 - p(\tau)] \left(\frac{\partial[\ln(1 - p(\tau))]}{\partial\tau} \right)^2 = \frac{[p'(\tau)]^2}{p(\tau)[1 - p(\tau)]}. \quad (\text{S2})$$

For traditional non-spectrally-resolved NOON-SI, the detector does not resolve the spectrum of the photons. The coincidence probability at time τ is then given by integrating the joint spectrum intensity $I(\omega_s, \omega_i, \tau)$ over ω_s and ω_i from zero to infinity as:

$$P_{NSR}(\tau) = \int_0^\infty \int_0^\infty I(\omega_s, \omega_i, \tau) d\omega_s d\omega_i = \frac{1}{2} \int_0^\infty \int_0^\infty |f(\omega_s, \omega_i)|^2 [1 + \cos(\omega_s + \omega_i)\tau] d\omega_s d\omega_i. \quad (\text{S3})$$

The differentiation of $P_{NSR}(\tau)$ is

$$P'_{NSR}(\tau) = -\frac{1}{2} \int_0^\infty \int_0^\infty |f(\omega_s, \omega_i)|^2 (\omega_s + \omega_i) \sin(\omega_s + \omega_i)\tau d\omega_s d\omega_i. \quad (\text{S4})$$

By substituting Eq. (S3) and Eq. (S4) into Eq. (S2), we obtain the Fisher information F_{NSR} as:

$$F_{NSR}(\tau) = \frac{[P'_{NSR}(\tau)]^2}{P_{NSR}(\tau)[1 - P_{NSR}(\tau)]}. \quad (\text{S5})$$

The Fisher information for non-spectrally-resolved NOON-SI in Fig.4 is plotted by using this equation.

1.2: Fisher information for spectrally-resolved NOON-SI

In the case of spectrally-resolved NOON-SI, the joint spectrum intensity $I(\omega_s, \omega_i, \tau)$ corresponds to the probability density that the signal and idler photons are detected at specific frequencies of ω_s and ω_i . Based on the assumption that the joint spectrum amplitude $f(\omega_s, \omega_i)$ of signal and idler photons generated from SPDC is already known, we obtain the corresponding null fringe $\tilde{I}(\omega_s, \omega_i, \tau)$ at specific frequencies as:

$$\tilde{I}(\omega_s, \omega_i, \tau) = |f(\omega_s, \omega_i)|^2 - I(\omega_s, \omega_i, \tau) = |f(\omega_s, \omega_i)|^2 \times \frac{1}{2} [1 - \cos(\omega_s + \omega_i)\tau]. \quad (\text{S6})$$

The amount of the information which is obtained at certain frequencies of ω_s and ω_i is given by these joint spectrum intensities in the form of Fisher information. Specially, Fisher information is given by integrating the amount of the information over ω_s and ω_i from zero to infinity as follows,

$$F_{SR}(\tau) = \int_0^\infty \int_0^\infty I(\omega_s, \omega_i, \tau) \left(\frac{\partial}{\partial \tau} I(\omega_s, \omega_i, \tau) \right)^2 + \tilde{I}(\omega_s, \omega_i, \tau) \left(\frac{\partial}{\partial \tau} \tilde{I}(\omega_s, \omega_i, \tau) \right)^2 d\omega_s d\omega_i \quad (\text{S7})$$

This equation can be further simplified as

$$F_{SR}(\tau) = \int_0^\infty \int_0^\infty |f(\omega_s, \omega_i)|^2 \times (\omega_s + \omega_i)^2 d\omega_s d\omega_i \quad (\text{S8})$$

Thus the Fisher information for spectrally-resolved NOON interference is constant and does not degrade in delay.